Int. J. Heat Mass Transfer. Vol. 19, pp. 1267–1272. Pergamon Press 1976. Printed in Great Britain

BUOYANCY INDUCED FLOWS IN A SATURATED POROUS MEDIUM ADJACENT TO IMPERMEABLE HORIZONTAL SURFACES

PING CHENG
Department of Mechanical Engineering, University of Hawaii, Honolulu, Hawaii

and

I-DEE CHANG
Department of Aeronautics & Astronautics, Stanford University, Stanford, California, U.S.A.

(*Received* 3 *January* 1976)

Abstract—Boundary-layer analysis is performed for the buoyancy-induced flows in a saturated porous medium adjacent to horizontal impermeable surfaces. Similarity solutions are obtained for the convective flow above a heated surface or below a cooled surface, where wall temperature is a power function of distance from the origin. Analytical expressions for boundary-layer thickness, local and overall surface heat flux are obtained. Applications to convective flow in a liquid-dominated geothermal reservoir are discussed.

NOMENCLATURE

A, constant defined by equation (6a);
C, specific heat of the convective fluid;
f, dimensionless stream function defined by equation (16);
g, acceleration due to gravity;
h, local heat-transfer coefficient;
$\bar{h}$, average heat-transfer coefficient defined by equation (33);
K, permeability of the porous medium;
k, thermal conductivity of the porous medium;
L, length of the heating or cooling surface;
Nu_x, local Nusselt number, $Nu_x = hx/k$;
$\overline{Nu}$, average Nusselt number, $\overline{Nu} = \bar{h}L/k$;
p, pressure;
Q, over-all heat-transfer rate;
q, local heat-transfer rate;
Ra, modified Rayleigh number, $Ra \equiv |\overline{T_w - T_\infty}|\rho_\infty g\beta KL/\mu\alpha$;
Ra_x, modified local Rayleigh number, $Ra_x \equiv \rho_\infty g\beta K|T_w - T_\infty|x/\mu\alpha$;
S, spanwise dimension;
T, temperature;
u, Darcy's velocity in x-direction;
v, Darcy's velocity in y-direction;
x, horizontal coordinate;
y, vertical coordinate.

Greek symbols

α, equivalent thermal diffusivity;
β, coefficient of thermal expansion;
δ_m, momentum boundary-layer thickness;
δ_T, thermal boundary-layer thickness;
η, dimensionless similarity variable defined by equation (15);
η_m, value of η at the edge of momentum boundary layer;
η_T, value of η at the edge of thermal boundary layer;
θ, dimensionless temperature defined by equation (17);
λ, constant defined by equation (6a);
μ, viscosity of convective fluid;
ρ, density of convective fluid;
ψ, stream function.

Subscripts

∞, condition at infinity;
w, condition at the wall.

1. INTRODUCTION

IT IS well known that if the temperature of a horizontal surface differs from that of the surrounding fluid, a vertical density gradient will be generated in the surrounding fluid which will induce a longitudinal pressure gradient. If the induced pressure gradient is greater than the buoyancy force, a convective movement in the direction of decreasing pressure is set up in the fluid adjacent to the surface. The buoyancy force in this situation is acting perpendicular to the direction of fluid motion. The problem has been studied theoretically by Stewartson [1], Gill [2], Rotem and Claasen [3], Pera and Gebhart [4], and Blanc and Gebhart [5], among others. In all of these papers, boundary-layer approximations are applied, and similarity solutions are obtained for wall temperature being a power function of distance from the leading edge.

The corresponding problem of buoyancy induced flow in a saturated porous medium adjacent to an impermeable wall has received relatively little attention. The first analytical paper dealing with this problem appears to be that of McNabb [6] who studied free convection in a saturated porous medium above a heated circular impermeable surface with wall tem-

perature being a step function with respect to the radius; boundary-layer approximations are invoked and approximate solutions are obtained. In the present paper, we shall study free convection in a saturated porous medium above a heated horizontal impermeable surface or below a cooled horizontal impermeable surface where wall temperature is a power function of distance from the origin. The boundary-layer approximations similar to those employed by Wooding [7], McNabb [6], and Cheng and Minkowycz [8] are invoked, and similarity solutions for the problem are obtained. The problem has important applications to convective flow above the heated bedrock or below the cooled caprock in a liquid-dominated geothermal reservoir.

2. ANALYSIS

Consider the problem of free convection in a saturated porous medium above a heated horizontal impermeable surface or below a cooled surface. The physical situation is shown in Fig. 1 where x and y are Cartesian coordinates in horizontal and vertical directions with positive y axis pointing toward the porous medium. The origin of the coordinate is chosen

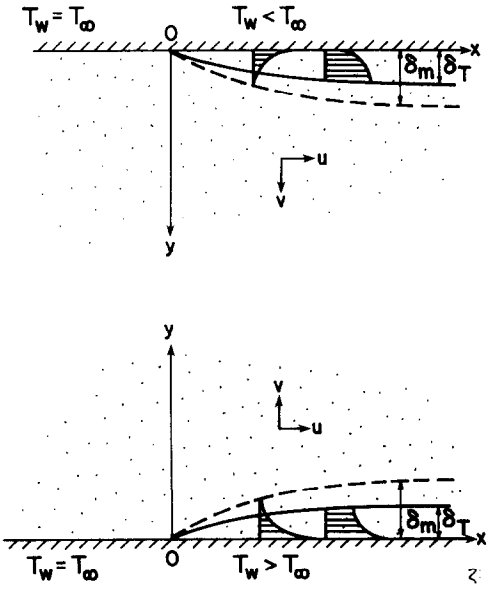

FIG. 1. Coordinate system.

at the point on the impermeable surface where wall temperature begins to deviate from that of the surrounding fluid. If we assume that (i) the convective fluid and the porous medium are everywhere in local thermodynamic equilibrium, (ii) the temperature of the fluid is everywhere below boiling point, (iii) properties of the fluid and the porous medium are constant, and (iv) the Boussinesq approximation is employed, the governing equations are given by

$$\frac{\partial u}{\partial x}+\frac{\partial v}{\partial y}=0, \tag{1}$$

$$u=-\frac{K}{\mu}\frac{\partial p}{\partial x}, \tag{2}$$

$$v=-\frac{K}{\mu}\left(\frac{\partial p}{\partial y}\pm\rho g\right), \tag{3}$$

$$u\frac{\partial T}{\partial x}+v\frac{\partial T}{\partial y}=\alpha\left(\frac{\partial^2 T}{\partial x^2}+\frac{\partial^2 T}{\partial y^2}\right), \tag{4}$$

$$\rho=\rho_\infty[1-\beta(T-T_\infty)], \tag{5}$$

where the "+" sign in equation (3) refers to the case of a heated plate facing upward (Fig. 1b) while the "−" sign refers to the case of a cooled plate facing downward (Fig. 1a). In equations (1)–(5), u and v are the velocity components in the horizontal and vertical directions, ρ, μ and β are the density, viscosity, and the thermal expansion coefficient of the convecting fluid, K is the permeability of the porous medium, $\alpha \equiv k/(\rho C)_f$ is the equivalent thermal diffusivity with k denoting the thermal conductivity of the saturated porous medium and $(\rho C)_f$ the product of density and specific heat of the convecting fluid. T, p and g are respectively the temperature, pressure, and the gravitational acceleration. The subscript "∞" refers to the condition at infinity.

The boundary conditions for the problem are

$$y=0,\quad T_w=T_\infty\pm Ax^\lambda,\quad v=0, \tag{6a, b}$$

$$y\to\infty,\quad T=T_\infty,\quad u=0, \tag{7a, b}$$

where $A>0$ and the "+" and "−" signs in equation (6a) are for a heated plate facing upward and for a cooled plate facing downward respectively. Equation (6a) shows that the prescribed wall temperature is a power function of distance from the origin.

The continuity equation is automatically satisfied by introducing the stream function ψ as

$$u=\frac{\partial\psi}{\partial y},\quad\text{and}\quad v=-\frac{\partial\psi}{\partial x}. \tag{8}$$

Eliminating p from equations (2) and (3) by cross differentiation, the resulting equation in terms of ψ is

$$\frac{\partial^2\psi}{\partial x^2}+\frac{\partial^2\psi}{\partial y^2}=\mp\frac{K\rho_\infty g\beta}{\mu}\frac{\partial T}{\partial x}. \tag{9}$$

In terms of ψ, equation (4) can be rewritten as

$$\frac{\partial^2 T}{\partial x^2}+\frac{\partial^2 T}{\partial y^2}=\frac{1}{\alpha}\left(\frac{\partial\psi}{\partial y}\frac{\partial T}{\partial x}-\frac{\partial\psi}{\partial x}\frac{\partial T}{\partial y}\right). \tag{10}$$

The appropriate boundary conditions for equations (9) and (10) are

$$y=0,\quad T_w=T_\infty\pm Ax^\lambda,\quad \frac{\partial\psi}{\partial x}=0, \tag{11a, b}$$

$$y\to\infty,\quad T=T_\infty,\quad \frac{\partial\psi}{\partial y}=0. \tag{12a, b}$$

3. SIMILARITY SOLUTION

From the numerical solutions for free convection in a geothermal reservoir [9], it is observed that thermal and momentum boundary layers exist along horizontal impermeable surfaces whenever wall temperature differs from that of the surrounding fluid. If boundary-

layer approximations are invoked, equations (9) and (10) become

$$\frac{\partial^2\psi}{\partial y^2} = \mp\frac{K\rho_\infty g\beta}{\mu}\frac{\partial T}{\partial x}, \tag{13}$$

and

$$\frac{\partial^2 T}{\partial y^2} = \frac{1}{\alpha}\left(\frac{\partial\psi}{\partial y}\frac{\partial T}{\partial x} - \frac{\partial\psi}{\partial x}\frac{\partial T}{\partial y}\right). \tag{14}$$

To seek similarity solutions to equations (13) and (14) with boundary conditions (11) and (12), we now introduce the following dimensionless variables

$$\eta = \left(\frac{K\rho_\infty g\beta A}{\mu\alpha}\right)^{1/3} yx^{(\lambda-2)/3} = (Ra_x)^{1/3}\frac{y}{x}, \tag{15}$$

$$\psi = \alpha\left[\frac{K\rho_\infty g\beta A}{\mu\alpha}\right]^{1/3} x^{(1+\lambda)/3} f(\eta) = \alpha(Ra_x)^{1/3} f(\eta), \tag{16}$$

$$\theta(\eta) = (T-T_\infty)/(T_w - T_\infty), \tag{17}$$

where $Ra_x \equiv \rho_\infty g\beta K|T_w - T_\infty|x/\mu\alpha$ is the modified local Rayleigh number.

In terms of new variables, it can be shown that the velocity components are given by

$$u = \alpha\left(\frac{K\rho_\infty g\beta A}{\mu\alpha}\right)^{2/3} x^{(2\lambda-1)/3} f'(\eta), \tag{18}$$

$$v = -\alpha\left[\frac{K\rho_\infty g\beta A}{\mu\alpha}\right]^{1/3}\left[\frac{\lambda-2}{3}\eta f' + \left(\frac{1+\lambda}{3}\right)f\right]x^{(\lambda-2)/3}. \tag{19}$$

Governing equations (13) and (14) in terms of the new variables are

$$f'' + \lambda\theta + \left(\frac{\lambda-2}{3}\right)\eta\theta' = 0, \tag{20}$$

$$\theta'' - \lambda\theta f' + \left(\frac{1+\lambda}{3}\right)f\theta' = 0, \tag{21}$$

with boundary conditions given by

$$\theta(0) = 1, \quad f(0) = 0, \tag{22a, b}$$

$$\theta(\infty) = 0, \quad f'(\infty) = 0, \tag{23a, b}$$

where the primes in equations (20)–(23) denote differentiation with respect to η.

4. RESULTS AND DISCUSSION

Equations (20) and (21) are two coupled non-linear differential equations for θ and f with two-point boundary conditions given by equations (22) and (23). Numerical solutions can be obtained by the Runge–Kutta method by first converting the boundary-value problem to an initial-value problem and with a systematic guessing of slopes at $\eta = 0$ by the shooting method. Results for f, f', θ and θ' vs η for selected values of λ are presented in Figs. 2–7.

The boundary-layer approximations used in the analysis are valid if (i) $\partial/\partial y \gg \partial/\partial x$ and (ii) $v \ll u$. From equation (15), it follows that $y/x = O(Ra_x^{-1/3})$. Furthermore, the ratio of equations (19) and (18) gives $v/u = O(Ra_x^{-1/3})$. Thus, the first and the second conditions

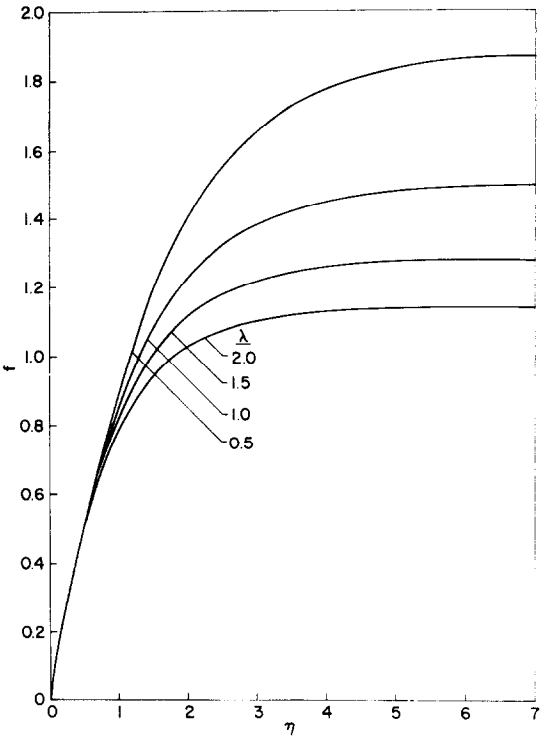

FIG. 2. Value of f vs η.

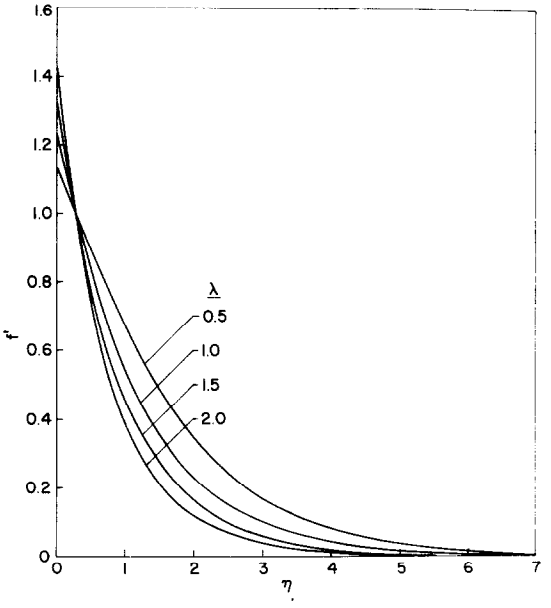

FIG. 3. Dimensionless velocity distribution vs η for selected values of λ.

are satisfied if Ra_x is large. Near the leading edge at $x = 0$, the boundary-layer approximations are not expected to be valid. The expressions for thermal and momentum boundary-layer thickness can be obtained if the edges of the boundary layers are defined as the points where θ or u/u_w (with u_w denoting the "slip velocity" along the wall) have a value of 0.01. From Figs. 3 and 4 we locate the edges of the boundary layers and denote these values by η_m and η_T. It follows

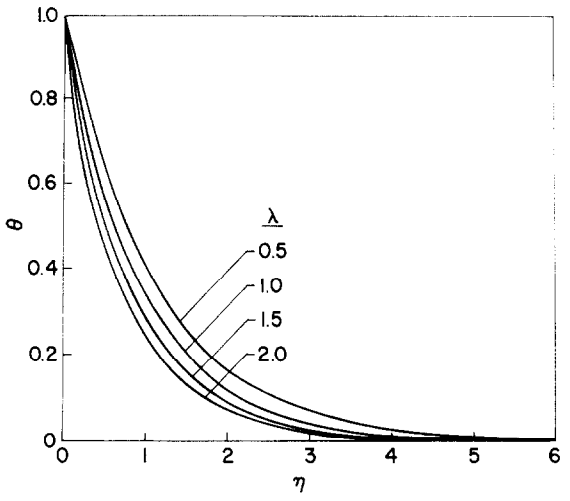

FIG. 4. Dimensionless temperature vs η for selected values of λ.

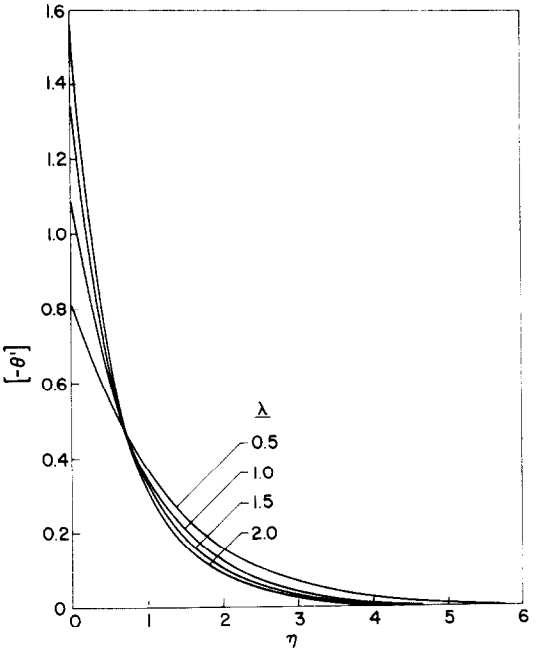

FIG. 5. Value of $[-\theta']$ vs η.

from equation (15) that

$$\frac{\delta_m}{x} = \frac{\eta_m}{(Ra_x)^{1/3}}, \tag{24a}$$

$$\frac{\delta_T}{x} = \frac{\eta_T}{(Ra_x)^{1/3}}, \tag{24b}$$

where the values of η_m and η_T for selected values of λ are tabulated in Table 1, which shows that the momentum boundary-layer thickness and the thermal boundary-layer thickness have about the same order of magnitude.

It is of interest to note that although $u \to 0$ outside the momentum boundary layer, the value of vertical velocity in general is not zero there. This can be seen

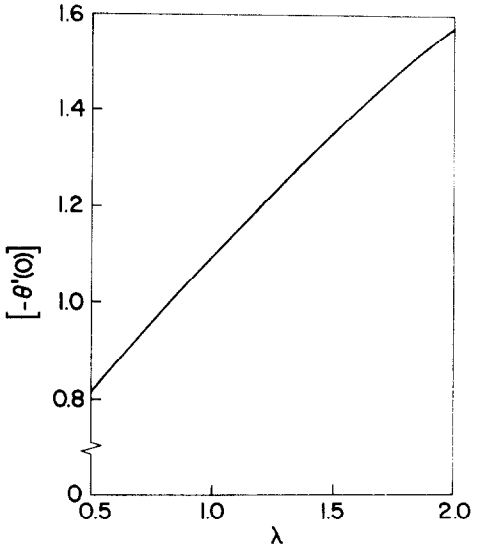

FIG. 6. Values of $Nu_x/(Ra_x)^{1/3}$ or $[-\theta(0)]$ vs λ.

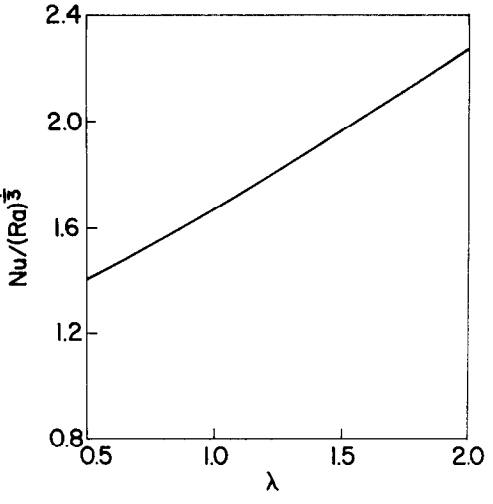

FIG. 7. Values of $\overline{Nu}/(Ra)^{1/3}$ vs λ.

Table 1. Values of $[-\theta'(0)]$, η_T, and η_m for selected values of λ

λ	$[-\theta'(0)]$	η_T	η_m
0.5	0.8164	5.0	6.4
1.0	1.099	4.5	5.4
1.5	1.351	4.0	4.4
2.0	1.571	3.7	3.8

from equation (19) with (23b) to give

$$v_\infty = -\frac{(1+\lambda)\alpha}{3}\left[\frac{K\rho_\infty g\beta A}{\mu\alpha}\right]^{1/3} f(\infty)x^{(\lambda-2)/3}, \tag{25}$$

which shows that v_∞ is negative if $\lambda > -1$, positive if $\lambda < -1$, and zero if $\lambda = -1$. Furthermore, the magnitude of v_∞ is increasing with x if $\lambda > 2$, decreasing with x if $\lambda < 2$, and independent of x if $\lambda = 2$. It is worth noting that the value $f(\infty)$ in equation (25) is positive and finite as shown in Fig. 2.

To obtain the pressure distribution, we substitute equations (2), (8) and (17) into equation (13) and integrate the resulting expression from $x = 0$ to x, and from y to $y = \infty$ to give

$$p(x, y) = \mp \rho_\infty g y + p_1(x, y), \tag{26a}$$

with

$$p_1(x, y) \equiv \mu\alpha\left[\frac{\rho_\infty g \beta A}{\mu\alpha}\right]^{2/3} x^{[2(\lambda+1)]/3} \int_\eta^\infty \theta(\eta)\,d\eta, \tag{26b}$$

where p_1 is the pressure induced by the density gradient. Along the wall at $y = 0$, equation (26a) reduces to

$$p(x, 0) = p_w(x) = \mu\alpha\left[\frac{\rho_\infty g \beta A}{\mu\alpha}\right]^{2/3} x^{[2(\lambda+1)]/3} \int_0^\infty \theta(\eta)\,d\eta, \tag{26c}$$

which shows that p_w is increasing, decreasing, or constant with respect to x depending on whether $\lambda > -1$, $\lambda < -1$, or $\lambda = -1$.

The local surface heat flux can be computed from

$$q = -k\left(\frac{\partial T}{\partial y}\right)_{y=0}. \tag{27}$$

With the aid of equations (17) and (15), equation (27) can be rewritten as

$$q(x) = kA^{4/3}\left[\frac{K\rho_\infty g \beta}{\mu\alpha}\right]^{1/3} x^{(4\lambda-2)/3}[-\theta'(0)], \tag{28}$$

which shows that $q(x)$ increases as x is increased if $\lambda > 1/2$; $q(x)$ decreases as x is increased if $\lambda < 1/2$; and $q(x)$ is constant if $\lambda = 1/2$.

We now examine the range of λ for which the problem is physically realistic. Since the wall temperature is different from that of the surrounding fluid at $x > 0$, both u and δ must be increasing or at least constant with respect to x. It follows from equations (18) and (25) that these conditions are satisfied if $1/2 \leqslant \lambda \leqslant 2$. Let's consider the variation of boundary-layer thickness, vertical velocity at infinity, local surface heat flux, induced pressure and horizontal velocity at the wall with respect to x, as given by equations (18) and (24)–(28), for the limiting cases of $\lambda = 1/2$ and $\lambda = 2$. The case of $\lambda = 1/2$ corresponds to the constant heat flux case where $u_w = \text{constant}$, $\delta \propto \sqrt{x}$, $v_\infty \propto 1/\sqrt{x}$, and $p_w \propto -x$. For the case of $\lambda = 2$, both δ and v_∞ are independent of x while $q \propto x^2$, $p_w \propto -x^2$, and $u_w \propto x$.

From the definition of the local Nusselt number $Nu_x \equiv hx/k = qx/k(T_w - T_\infty)$ (where h is the local heat-transfer coefficient) and with the aid of equation (28), we have

$$\frac{Nu_x}{(Ra_x)^{1/3}} = [-\theta'(0)], \tag{29}$$

which is presented for selected values of λ in Table 1 and plotted in Fig. 6.

The overall surface heat-transfer rate for a rectangular surface with a length L and a width S can be computed from

$$Q = S\int_0^L q(x)\,dx, \tag{30}$$

which can be integrated explicitly after $q(x)$, given by equation (28), has been substituted in equation (30) to give

$$Q = \left(\frac{3}{4\lambda+1}\right)[-\theta'(0)]SkA^{4/3}\left[\frac{\rho_\infty g \beta K}{\mu\alpha}\right]^{1/3} L^{(4\lambda+1)/3}. \tag{31}$$

The average Nusselt number is defined by $\overline{Nu} = \bar{h}L/k$ where the average heat-transfer coefficient $\bar{h}$ depends on the choice of the temperature difference between the wall and the temperature of the fluid away from the wall. If the temperature difference is based on the mean temperature difference defined by

$$(\overline{T_w - T_\infty}) = \frac{1}{L}\int_0^L (T_w - T_\infty)\,dx = \frac{AL^\lambda}{1+\lambda} = \frac{(T_w - T_\infty)_L}{1+\lambda}, \tag{32}$$

and

$$Q = \bar{h}(\overline{T_w - T_\infty})SL, \tag{33}$$

then, the average Nusselt number is given by

$$\frac{\overline{Nu}}{(Ra)^{1/3}} = \frac{3(1+\lambda)^{4/3}}{(1+4\lambda)}[-\theta'(0)], \tag{34}$$

where $Ra \equiv |\overline{T_w - T_\infty}|\rho_\infty g \beta K L/\mu\alpha$. Equation (34) for different values of λ is presented in Table 2 and in Fig. 7.

Table 2. Values of $Nu/(Ra)^{1/3}$

λ	$Nu/(Ra)^{1/3}$
0.5	1.402
1.0	1.662
1.5	1.965
2.0	2.266

To gain some feeling of the order of magnitude of various physical quantities in a geothermal application, consider an upward facing heated horizontal impermeable surface, 1 km by 1 km, with a wall temperature increasing from 288°K at $x = 0$ to 573°K at $x = 1$ km according to a power law variation given by equation (6a). For numerical computations the following physical properties are used: $\beta = 2.8 \times 10^{-4}$/K, $\rho_\infty = 0.92 \times 10^6$ g/m^3, $C = 4.2 \times 10^3$ J/kg K, and $k = 2.4$ W/m K. The value of μ is a strong function of temperature varying from 0.54×10^{-3} Ns/m^2 at 288 K to 0.042×10^{-3} Ns/m^2 at 573 K, whereas the value of K depends on the locality ranging from 10^{-14} m^2 at Wairakei, New Zealand, to 10^{-10} m^2 at Hawaii. If the value of $\mu = 0.54 \times 10^{-3}$ Ns/m^2 and $K = 10^{-12}$ m^2 are used, the boundary-layer thickness at $x = 1$ km and the total heat-transfer rate for selected λ are presented in Table 3. It should be noted that if the values of $\mu = 0.042 \times 10^{-3}$ Ns/m^2 and $K = 10^{-10}$ m^2 are used, the boundary-layer thickness will be considerably thinner with an associated increase in heat-transfer rate.

Table 3. Values of δ_m and δ_T at $x = 1$ km as well as Q for selected values of λ

λ	δ_m	δ_T	Q
0.5	503 m	379 m	7.2 MW
1.0	434 m	341 m	5.8 MW
1.5	364 m	310 m	5.1 MW
2.0	325 m	279 m	4.6 MW

5. CONCLUDING REMARKS

The foregoing analysis is based on the boundary-layer approximations which are applicable for large Rayleigh numbers. The analytical expressions for total surface heat transfer can be used for an approximate estimate of energy transfer rate between a horizontal surface to the surrounding saturated porous medium when the temperature of the impermeable surface is different from that of the surrounding fluid. The first author (P. Cheng) has extended the present analysis to an axisymmetric flow in a porous medium heated or cooled by a circular impermeable surface [10].

Acknowledgement—The authors would like to take this opportunity to thank Mr. W. C. Chau for his assistance in the numerical computations. This study is part of the Hawaii Geothermal Project funded in part by the RANN program of the National Science Foundation of the United States (Grant No. GI-38319), the Energy Research and Development Administration of the United States (Grant No. E(04-3)-1093), and by the State and County of Hawaii.

REFERENCES

1. K. Stewartson, On the free convection from a horizontal plate, *Z. Angew. Math. Phys.* **9**, 276–281 (1958).
2. W. N. Gill, D. W. Zeh and E. D. Casal, Free convection on a horizontal plate, *Z. Angew. Math. Phys.* **16**, 539–541 (1965).
3. Z. Rotem and L. Claussen, Natural convection above unconfined horizontal surfaces, *J. Fluid Mech.* **38**, 173–192 (1969).
4. L. Pera and B. Gebhart, Natural convection flows adjacent to horizontal surfaces resulting from the combined buoyancy effects of thermal and mass diffusion, *Int. J. Heat Mass Transfer* **15**, 269–278 (1972).
5. P. Blanc and B. Gebhart, Buoyancy induced flows adjacent to horizontal surfaces, in *Proceedings of the 5th International Heat Transfer Conference, Tokyo, Japan, 3–7 September* 1974. A.I.Ch.E., New York (1974).
6. A. McNabb, On convection in a saturated porous medium, in *Proceedings of the 2nd Australian Conference on Hydraulics and Fluid Mechanics*, pp. C161–C171. The University of Auckland Press, New Zealand (1965).
7. R. A. Wooding, Convection in a saturated porous medium at large Rayleigh number or Peclet number, *J. Fluid Mech.* **15**, 527–544 (1963).
8. P. Cheng and W. J. Minkowycz, Similarity solutions for free convection about a dike, Hawaii Geothermal Project, Engineering Program, Technical Report No. 10 (October 1975).
9. P. Cheng, K. C. Yeung and K. H. Lau, Numerical solutions for steady free convection in island geothermal reservoirs, in *Proceedings of* 1975 *International Seminar on Future Energy Production—Heat and Mass Transfer Problems*. Hemisphere, Washington, D.C. (1965).
10. P. Cheng and W. C. Chau, Similarity solutions for convection of ground-water adjacent to horizontal impermeable surfaces with axisymmetric temperature distribution, Hawaii Geothermal Project, Engineering Program, Technical Report No. 14 (April 1976).

ECOULEMENT DE CONVECTION NATURELLE DANS UN MILIEU POREUX SATURE ADJACENT A DES SURFACES IMPERMEABLES HORIZONTALES

Résumé—L'écoulement produit par les forces de gravité dans un milieu poreux saturé adjacent à des surfaces imperméables horizontales est étudié suivant une analyse du type couche-limite. Des solutions en similitude sont obtenues pour l'écoulement convectif sur une surface chauffée ou sous une surface refroidie lorsque la température de paroi est une fonction puissance de la distance à l'origine. On donne des expressions analytiques des épaisseurs de couche limite et des flux de chaleur pariétaux locaux et globaux. Des applications à l'écoulement convectif dans un réservoir géothermique à prédominance liquide sont également discutées.

FREIE KONVEKTIONSSTRÖMUNGEN IN EINEM GESÄTTIGTEN, PORÖSEN MEDIUM, DAS AN UNDURCHLÄSSIGE, WAAGERECHTE OBERFLÄCHEN ANGRENZT

Zusammenfassung—Für freie Konvektionsströmungen in einem gesättigten, porösen Medium, das an waagerechte, undurchlässige Oberflächen angrenzt, wird eine Grenzschichtanalyse durchgeführt. Ähnlichkeitslösungen ergeben sich für die Konvektionsströmung oberhalb einer erwärmten Oberfläche oder unterhalb einer gekühlten Fläche, wo die Wandtemperatur eine Potenzfunktion des Abstands vom Ursprung darstellt. Analytische Ausdrücke lassen sich für die Grenzschichtdicke, den örtlichen und integralen Wärmestrom erhalten. Anwendungen auf konvektive Strömungen in einem flüssigkeitsdominierten geothermischen Speicher werden diskutiert.

СВОБОДНЫЕ ТУРБУЛЕНТНЫЕ ТЕЧЕНИЯ В НАСЫЩЕННОЙ ПОРИСТОЙ СРЕДЕ ВБЛИЗИ НЕПРОНИЦАЕМЫХ ГОРИЗОНТАЛЬНЫХ ПОВЕРХНОСТЕЙ

Аннотация — С помощью теории пограничного слоя рассматриваются свободные турбулентные течения в насыщенной пористой среде вблизи непроницаемых горизонтальных поверхностей. Получены сходные решения для конвективного потока над нагреваемой поверхностью, когда температура стенки является степенной функцией расстояния от начала координат. Получены аналитические выражения для толщины пограничного слоя, локального и суммарного теплового потока на поверхности. Обсуждаются приложения к конвективному течению в жидкостном геотермическом резервуаре.